Measurements of Kondo and Spin Splitting in Single-Electron Transistors

A. Kogan,[1,*] S. Amasha,[1] D. Goldhaber-Gordon,[1,†] G. Granger,[1] M. A. Kastner,[1,‡] and Hadas Shtrikman[2]

[1]*Department of Physics, Massachusetts Institute of Technology, Cambridge, Massachusetts 02139, USA*
[2]*Braun Center for Submicron Research, Weizmann Institute of Science, Rehovot, 76100 Israel*

We measure the spin splitting in a magnetic field B of localized states in single-electron transistors using a new method, inelastic spin-flip cotunneling. Because it involves only internal excitations, this technique gives the most precise value of the Zeeman energy $\Delta = |g|\mu_B B$. In the same devices we also measure the splitting with B of the Kondo peak in differential conductance. The Kondo splitting appears only above a threshold field as predicted by theory. However, the magnitude of the Kondo splitting at high fields exceeds $2|g|\mu_B B$ in disagreement with theory.

The Kondo state, formed when conduction electrons screen a magnetic impurity, has received new attention since its observation in nanostructures, because it is a spin-entangled state of the many-electron system. While the equilibrium properties of Kondo systems are described quantitatively by theory, nonequilibrium Kondo phenomena have proved harder to understand. Single-electron transistors (SETs) provide the unique possibility of exploring these nonequilibrium phenomena. An SET consists of a confined droplet of electrons, called an artificial atom or a quantum dot, coupled by tunnel barriers to two conducting leads, called the source and the drain. The electrochemical potential of the dot, as well as the coupling between the dot and the leads, can be tuned by changing voltages on electrodes. The Kondo effect in SETs [1–4] occurs because a dot in a nonzero spin state coupled to its leads is analogous to a magnetic impurity coupled to the electrons in a host metal. Kondo correlations develop because the dot spin is screened by the spins of electrons in the leads. In an SET the Kondo state can be studied out of equilibrium by applying a dc voltage V_{ds} between the source and the drain.

Nonequilibrium Kondo physics is probed by the measurement of the splitting of the Kondo peak in differential conductance as a function of magnetic field B [5–8]. Meir *et al.* [5] predict that in a magnetic field the Kondo peaks occur at $eV_{ds} = \pm \Delta$. Here $\Delta = |g|\mu_B B$ is the Zeeman energy for spin splitting and $\mu_B = 58$ μeV/T is the Bohr magneton. Cronenwett *et al.* [2] have measured the splitting of a Kondo peak and have found good agreement with this prediction, using $g = -0.44$ for bulk GaAs. However, more recent calculations by Costi [6] predict that the Kondo peak splitting should appear only above a critical magnetic field, and Moore and Wen [7] predict that the splitting should be smaller than 2Δ at all fields.

Here we report measurements comparing the Kondo peak splitting to Δ in SETs. Using electron addition spectroscopy and a new, more precise method, inelastic spin-flip cotunneling, we determine Δ and hence the g factor of our SETs. We find that the Kondo splitting appears only above a critical field as predicted by theory.

However, the magnitude of the Kondo splitting at high fields is noticeably *larger* than 2Δ, contrary to theoretical predictions.

The two SETs we have studied are similar to those used by Goldhaber-Gordon *et al.* [1,9], and details about the AlGaAs/GaAs heterostructure can be found in the latter references. A two dimensional electron gas (2DEG) is formed at the AlGaAs/GaAs interface with an electron density of 8.1×10^{11} cm^{-2} and a mobility of 10^5 cm$^2/V$ s at 4.2 K. Magnetotransport shows that only one sub-band of the 2DEG is occupied. Electron-beam lithography is used to define the gate electrodes shown in the inset of Fig. 1(c). Applying a negative voltage to these electrodes depletes the 2DEG underneath them and forms an artificial atom of about 50 electrons isolated by two tunnel barriers from the remaining 2DEG regions, the source and drain leads. The voltage on the gate electrode g is denoted V_g.

The two SETs were studied in different dilution refrigerators. SET 1 was measured in a Leiden Cryogenics 400 μW dilution refrigerator with a 14 T magnet and a lowest electron temperature of 20–30 mK. The sample was aligned so that the 2DEG was parallel to the magnetic field to better than 0.5°. SET 2 was measured in a 75 μW Oxford Instruments dilution refrigerator with an 8 T magnet and a lowest electron temperature of about 110 mK. This sample could only be aligned parallel to the magnetic field to within a few degrees. To measure the differential conductance dI/dV_{ds}, we added a small sinusoidal modulation to V_{ds} and measured the resulting current with a preamplifier and a lock-in amplifier.

One way to measure the Zeeman splitting of orbital levels in an SET is electron addition spectroscopy [10,11]. Figure 1(a) shows a plot of dI/dV_{ds} as a function of V_{ds} and V_g while Fig. 1(b) shows dI/dV_{ds} at the value of V_g marked on Fig. 1(a) with a dashed line, for which the occupancy of the dot is even. As we increase V_{ds} at this fixed V_g, we lower the Fermi energy of the drain lead. The first peak in dI/dV_{ds} occurs when the Fermi energy of the drain aligns with the higher energy state of the spin split
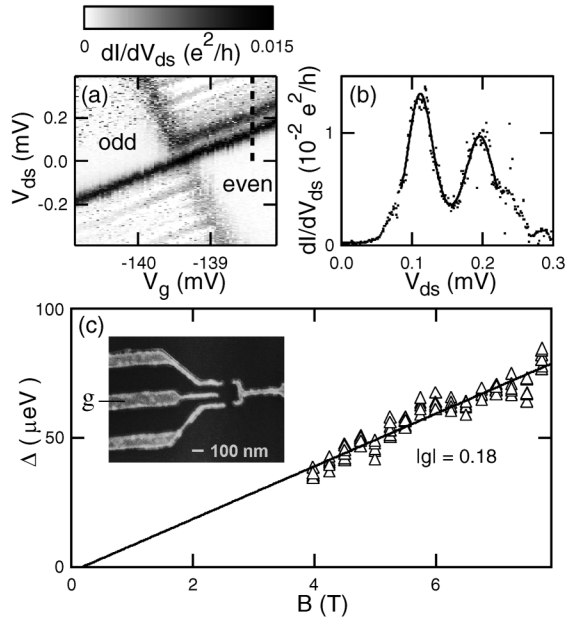
FIG. 1. (a) Differential conductance as a function of V_{ds} and V_g at $B = 7.25$ T for SET 2. The odd and even Coulomb valleys are labeled. (b) Differential conductance as a function of drain-source voltage at the gate voltage marked by the dashed line in (a). The dots denote data while the solid line shows a fit to the sum of two $\cosh^{-2}$ functions. (c) Zeeman splitting as a function of magnetic field determined by fitting curves like that shown in (b). The solid line shows a fit to the data to determine $|g|$. The inset shows an electron micrograph of an SET similar to those we studied.

orbital state in the SET. Since even occupancy implies *both* spin states are filled at $V_{ds} = 0$, a second peak appears when the lower energy spin state enters the transport window. The separation of the two peaks is $\Delta/e(1 - \alpha_d)$, where α_d is the ratio of the dot-drain capacitance to the total capacitance. The $(1 - \alpha_d)$ factor arises because applying a positive voltage to the drain slightly lowers the energies of the levels in the dot.

To find the peak splitting we fit data like those in Fig. 1(b) to the sum of two $\cosh^{-2}$ functions; the specific form chosen does not affect the measurement of the splitting. Using the slopes of a Coulomb-blockade diamond, part of which is shown in Fig. 1(a), we determine $\alpha_d = 0.15 \pm 0.02$ and hence Δ. Figure 1(c) shows Δ as a function of B. At each field we fit several traces like that in Fig. 1(b). The scatter in the data arises because charge fluctuations near the SET are equivalent to gate voltage fluctuations and cause fluctuations in the peak positions. Fitting the data in Fig. 1(c) to a line gives $|g| = 0.18 \pm 0.04$.

We have developed a new, more precise method of measuring Δ using inelastic spin-flip cotunneling. Although resonant tunneling is prohibited in the Coulomb-blockade regime, an electron can tunnel through the SET via a virtual intermediate state, a process known as cotunneling [12]. Cotunneling can proceed elastically and leave

the SET in its ground state, or inelastically, leaving it in an excited state. De Franceschi *et al.* [13] observed inelastic cotunneling through an excited *orbital* state of an SET with an even number of electrons. In our experiments the ground state has an odd number of electrons and the role of the excited state is played by the higher energy spin state. The elastic and inelastic cotunneling processes are illustrated in Fig. 2(a)–2(d). If $|eV_{ds}| < \Delta$ only the elastic process is possible, but if $|eV_{ds}| \geq \Delta$ both the elastic and inelastic processes are possible and we expect steps in dI/dV_{ds} at $|eV_{ds}| = \Delta$.

This behavior is illustrated in Fig. 3(a) and 3(b). Note that the spin-flip cotunneling gap is independent of gate voltage and, as shown in Fig. 4(a), is only observed in a magnetic field. This is in contrast to cotunneling features associated with excited orbital states, like those in the Coulomb valley on the far left in Fig. 3(a), which depend on V_g because changing the gate voltage alters the shape of the confining potential [13,14]. The orbital cotunneling features are also present at $B = 0$. To our knowledge, this is the first observation of the threshold for spin-flip cotunneling in an SET.

Increasing the temperature broadens the inelastic cotunneling threshold. Lambe and Jaklevic [15] have shown that for an inelastic process with negligible intrinsic width the line shape is given by

$$\frac{dI}{dV_{ds}} = A_e + A_i \left[F\left(\frac{eV_{ds} + \Delta}{k_B T}\right) + F\left(-\frac{eV_{ds} - \Delta}{k_B T}\right) \right]. \tag{1}$$

In this equation, A_e is the conductance from elastic cotunneling and A_i describes the additional contribution from inelastic cotunneling. F is a function defined by $F(x) = [1 + (x - 1)\exp(x)]/[\exp(x) - 1]^2$. This line shape has steps centered at $V_{ds} = \pm\Delta/e$ with width $5.4 k_B T/e$. A fit to Eq. (1) is shown as the solid line in
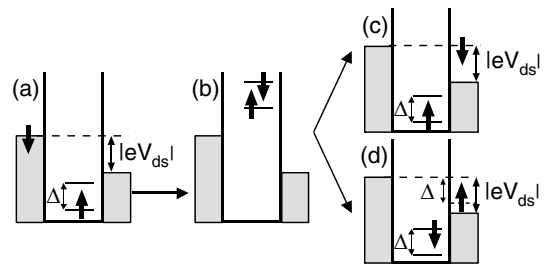

FIG. 2. Cotunneling processes through a Zeeman split orbital, which can occur when the dot is in the Coulomb-blockade regime with an odd number of electrons as in (a). We take spin up to be the lower energy state. A spin-down electron from the lead can tunnel onto the dot forming the virtual intermediate state shown in (b). For any value of V_{ds}, the spin-down electron can tunnel off the dot as shown in (c), resulting in elastic cotunneling. If $|eV_{ds}| \geq \Delta = |g|\mu_B B$, the spin-up electron can also tunnel off the dot resulting in inelastic cotunneling as shown in (d).
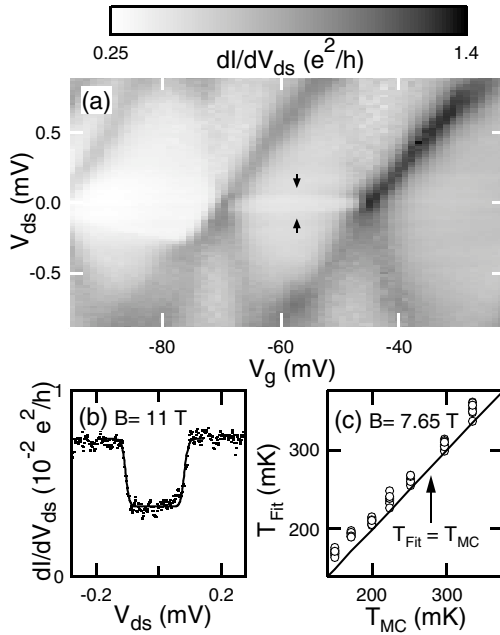
FIG. 3. (a) Differential conductance as a function of V_{ds} and V_g at $B = 8$ T for SET 1. The inelastic spin-flip cotunneling gap is in the middle of the center diamond and is marked by arrows. (b) Differential conductance as a function of drain-source voltage in the middle of the Coulomb valley for the same sample as in (a), but with different voltages on the electrodes and $B = 11$ T. The dots are the data and the solid line is a fit described in the text. (c) Temperatures extracted from fitting the cotunneling gap of SET 2 at $B = 7.65$ T. The horizontal axis is the mixing chamber temperature T_{MC} and the vertical axis is the temperature T_{Fit} extracted from fitting the gap as discussed in the text. The line shows $T_{MC} = T_{Fit}$.

Fig. 3(b) and is in excellent agreement with the data. Figure 3(c) shows the temperature T_{Fit} extracted from fits to data taken at different temperatures with SET 2. The sharpest cotunneling step that we have observed [shown in Fig. 3(b)] is for SET 1 and has width 22 μeV. This can be used to place a lower bound on the spin decoherence time because the intrinsic width of the cotunneling step is inversely proportional to the decoherence time.

Figure 4(a) shows the evolution with field of a cotunneling feature in SET 2. The splittings Δ from fits to Eq. (1) are plotted as functions of B in Fig. 4(b). Fitting these data to a line gives $|g| = 0.16 \pm 0.02$, consistent with the value from addition spectroscopy but with greater precision. Measurements for SET 1 in high magnetic fields, shown in Figs. 4(c) and 4(d), give $|g| = 0.152 \pm 0.006$, consistent with the value for SET 2. The inelastic cotunneling method, which measures the spectrum of internal excitations of the dot, is more precise than electron addition spectroscopy for two reasons. First, the cotunneling spectrum is independent of the chemical potential of the dot, making the splitting insensitive to small charge fluctuations near the SET. Second, the cotunneling method is inherently more pre-
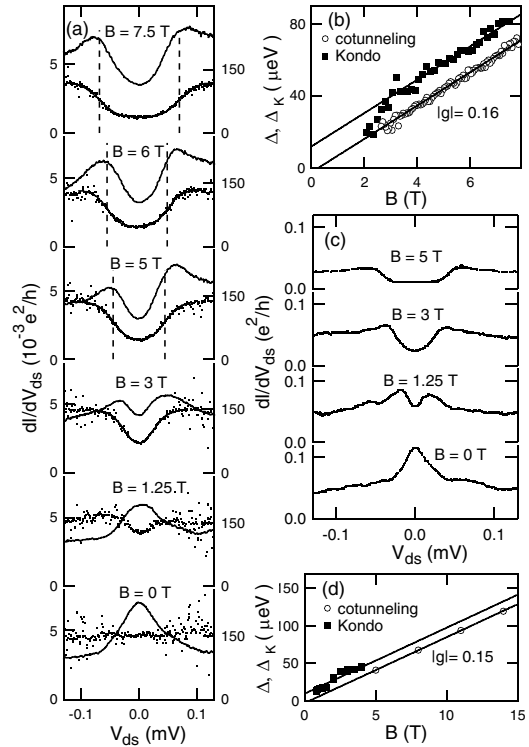
FIG. 4. (a) Evolution of a cotunneling gap (dots) and a Kondo peak (solid line) with increasing magnetic field in SET 2. The vertical scale on the left (right) is for the cotunneling data (Kondo data). For the cotunneling data, the coupling to the leads was reduced so that no Kondo peak was seen at zero field at the measurement temperature $T \approx 110$ mK. The solid lines through the cotunneling data at high fields are examples of fits to Eq. (1). The dashed lines at the three highest fields mark the center of the cotunneling edge; the lines are 2Δ apart. (b) Splittings from cotunneling gaps (open circles) and Kondo peaks (solid squares) from SET 2. The solid line through the cotunneling data is a linear fit. The line through the Kondo data is the result of fixing the slope at the value obtained from the cotunneling data and fitting the data above 3 T to extract the intercept. (c) Evolution of a Kondo peak into a cotunneling gap with increasing magnetic field in SET 1. The solid line in the 5 T trace shows a fit as described in the text. (d) Splittings from the cotunneling gaps and Kondo peaks for SET 1. The Kondo splitting is determined at low field and the cotunneling gap at high field, but all other parameters are unchanged. We fit the data with lines the same way as for (b).

cise because its intrinsic width is smaller than the width of the charging peak, which is determined by the coupling to the leads and is approximately $\Gamma = 35$ μeV for SET 2 in Fig. 1.

The splitting of the Kondo peak at high fields is larger than the cotunneling gap, as can be seen, for example, from the data in Fig. 4(a). To compare our findings to theory, we follow Moore and Wen [7] who identify the field-induced splitting between the two peaks in their calculated spectral function with the splitting in V_{ds} between the peaks in dI/dV_{ds}. We define Δ_K/e as half the separation in V_{ds} between the two peaks. Figure 4(b)

shows Δ_K for SET 2 from data like those shown in Fig. 4(a). There is a clear offset between Δ_K and the cotunneling data at high fields; fitting the data above 3 T to a line with $|g|$ fixed at the value obtained from cotunneling gives an offset of 12 ± 1 μeV.

The Kondo peak evolves smoothly into a cotunneling threshold with increasing B when there is an odd number of electrons in the dot. Figure 4(c) shows this evolution for SET 1. Note that the values of Δ in Fig. 4(d) are extracted from the high-field data for which the Kondo peak is absent. The Δ_K are extracted from the low-field data and are plotted in Fig. 4(d). We fit the data to a line with the slope fixed at the value obtained from the cotunneling data points, $|g| = 0.152$. The fit gives a y intercept of 10 ± 2 μeV, similar to the result for SET 2. Note that in contrast to the Kondo data, both the addition spectroscopy and cotunneling measurements extrapolate to zero within the errors at $B = 0$. Contrary to theoretical predictions [7], Δ_K is *larger* than $|g|\mu_B B$.

Another feature of the Kondo data is that the splitting only appears above a threshold magnetic field. For example, the 1.25 T data in Fig. 4(a) shows no evidence of splitting. The data for Δ_K in Fig. 4(b) shows a threshold for splitting near 2 T, which is where $|g|\mu_B B/k_B \approx T_K \approx$ 300 mK. Costi [6] predicts a threshold field for the Kondo splitting. In this respect our results are consistent with theory.

The value of $|g|$ in our SETs is 0.16, much smaller than the bulk GaAs value of 0.44. The small g factor may arise because the electron density in our SETs is much larger than in typical devices. Variations in the g factor with density have previously been observed in AlGaAs/GaAs heterostructures [16–20]. We believe our small value results from penetration of the electrons into the $Al_{0.3}Ga_{0.7}As$ which has $g = +0.4$, and the large 2DEG density in our SETs enhances this effect. Linearly extrapolating the results of Jiang and Yablonovitch [19] gives a change in $|g|$ that is about half of that we observe. We plan a more realistic calculation to test this hypothesis more carefully.

The observation that $\Delta_K > |g|\mu_B B$ is surprising. Moore and Wen [7] predict that $\Delta_K < |g|\mu_B B$ at all B, whereas we find that $\Delta_K > |g|\mu_B B$ by ≈ 10 μeV at high fields. Our results differ from those of Goldhaber-Gordon *et al.* [1]. However, the measurements reported by Goldhaber-Gordon *et al.* are taken with the magnetic field normal to the 2DEG and could involve effects from the orbital motion of the electrons. Such effects are not considered by Moore and Wen [7] and are eliminated in the present experiments by orienting the 2DEG parallel to the magnetic field. One might ask if elastic cotunneling forms a background that could explain our observations. Using zero field data like those in Fig. 4(a), only over a wider range of V_{ds}, we fit the cotunneling conductance outside the Kondo peak region to a parabola and subtract this from our Kondo splitting data from SET 2. This decreases the high-field offset by about 5%, which does not affect our conclusions. However, such a subtraction is not well motivated since elastic and inelastic cotunneling processes contribute coherently to the Kondo correlations. Thus the observation that $\Delta_K > |g|\mu_B B$ is not understood and suggests that more theoretical analysis of the non-equilibrium Kondo problem is important.

*Current address: Department of Physics, University of Cincinnati, Cincinnati, OH 45221-0011, USA

†Current address: Geballe Laboratory for Advanced Materials, McCullough Building, Room 346, 476 Lomita Mall, Stanford, CA 94305-4045, USA

‡Electronic address: mkastner@mit.edu

[1] D. Goldhaber-Gordon *et al.*, Nature (London) **391**, 156 (1998).
[2] S. Cronenwett *et al.*, Science **281**, 540 (1998).
[3] L. I. Glazman and M. E. Raikh, JETP Lett. **47**, 452 (1988).
[4] T. K. Ng and P. A. Lee, Phys. Rev. Lett. **61**, 1768 (1988).
[5] Y. Meir *et al.*, Phys. Rev. Lett. **70**, 2601 (1993).
[6] T. A. Costi, Phys. Rev. Lett. **85**, 1504 (2000).
[7] J. E. Moore and X.-G. Wen, Phys. Rev. Lett. **85**, 1722 (2000).
[8] A. Rosch *et al.*, Phys. Rev. Lett. **90**, 076804 (2003).
[9] D. Goldhaber-Gordon *et al.*, Phys. Rev. Lett. **81**, 5225 (1998).
[10] R. Potok *et al.*, Phys. Rev. Lett. **91**, 016802 (2003).
[11] R. Hanson *et al.*, Phys. Rev. Lett. **91**, 196802 (2003).
[12] D. V. Averin and Yu. V. Nazarov, in *Single Charge Tunneling*, edited by H. Grabert and M. H. Devoret, NATO ASI Series B 294 (Plenum, New York, 1992), p. 217.
[13] S. De Franceschi *et al.*, Phys. Rev. Lett. **86**, 878 (2001).
[14] A. Kogan *et al.*, Phys. Rev. B **67**, 113309 (2003).
[15] J. Lambe and R. C. Jaklevic, Phys. Rev. **165**, 821 (1968).
[16] D. Stein *et al.*, Phys. Rev. Lett. **51**, 130 (1983).
[17] M. Dobers *et al.*, Phys. Rev. B **38**, 5453 (1988).
[18] M. J. Snelling *et al.*, Phys. Rev. B **44**, 11345 (1991).
[19] H. W. Jiang and E. Yablonovitch, Phys. Rev. B **64**, 041307(R) (2001).
[20] G. Salis *et al.*, Nature (London) **414**, 619 (2001).